JOC Article

Probing the Dynamic Environment-Associated Conformational Conversion from Secondary to Supersecondary Structures in Oligo(phenanthroline dicarboxamide)s

Hai-Yu Hu,[†,‡] Wei Xue,[†,‡] Zhi-Qiang Hu,[†] Jun-Feng Xiang,[†] Chuan-Feng Chen,*[,†] and Sheng-Gui He*[,†]

Beijing National Laboratory for Molecular Sciences, CAS Key Laboratory of Molecular Recognition and Function, Institute of Chemistry, Chinese Academy of Sciences, Beijing 100190, China, and Graduate School, Chinese Academy of Sciences, Beijing 100049, China

cchen@iccas.ac.cn

Received March 27, 2009

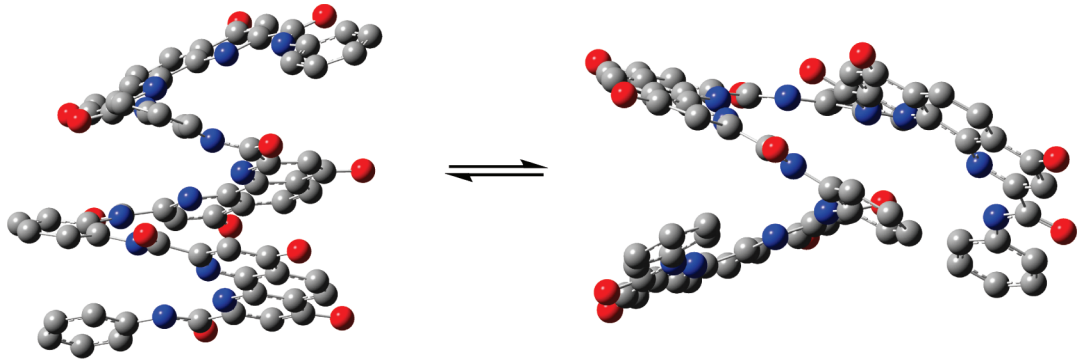

The special structural features of the oligo(phenanthroline dicarboxamide)s and their dynamic environment-associated conformational conversion from secondary helical structure to supersecondary helix-turn structure, owing to the conversion of the CONH bond from s-cis form to s-trans form, have been experimentally and theoretically characterized by X-ray crystallographic, variable-temperature ^{1}H NMR, variable-temperature circular dichroism techniques, and computational studies. It has been demonstrated that the solvent effects together with intramolecular hydrogen bonds and $\pi-\pi$ stacking play a key role in stabilizing both the secondary and supersecondary structures. Furthermore, by introducing the intramolecular F···H−N hydrogen bond to restrict the rotation about the CONH−aryl bonds, the oligomers **6** and **7** have been synthesized, which showed well-defined and predictable secondary helical conformations in solution and in the solid state.

Introduction

The long-held tenet of protein folding that "one sequence determines one structure" was breaking down to some extent, and some sequences encode two or more folded states,[1] which was referred to as structural duality.[2] Meanwhile, protein folding and stability became a subject that has generated intense research interest with the recognition that disease states arise from aberrant folding or stability.[3]

The remarkable features of proteins have prompted chemists to investigate oligomers capable of adopting well-defined, compact conformations for mimicking the structures and functions of biological macromolecules. In the past decade, synthetic helical foldamers[4,5] have attracted great attention in mimicking the conformational behavior of biopolymers and showing potential applications in molecular recognition, sensing, trans-

[†] Beijing National Laboratory for Molecular Sciences, CAS Key Laboratory of Molecular Recognition and Function, Institute of Chemistry, Chinese Academy of Sciences.

[‡] Graduate School, Chinese Academy of Sciences.

(1) (a) Minor, D. L.; Kim, P. S. *Nature* **1996**, *380*, 730–734. (b) Kuznetsov, I. B.; Rackovsky, S. *Protein Sci.* **2003**, *12*, 2420–2433.

(2) (a) Pandya, M. J.; Cerasoli, E.; Joseph, A.; Stoneman, R. G.; Waite, E.; Woolfson, D. N. *J. Am. Chem. Soc.* **2004**, *126*, 17016–17024. (b) Ciani, B.; Hutchinson, E. G.; Sessions, R. B.; Woolfson, D. N. *J. Biol. Chem.* **2002**, *277*, 10150–10155.

(3) (a) Rochet, J. C.; Lansbury, P. T. *Curr. Opin. Struct. Biol.* **2000**, *10*, 60–68. (b) Cohen, F. E. *J. Mol. Biol.* **1999**, *293*, 313–320. (c) Carrell, R. W.; Gooptu, B. *Curr. Opin. Struct. Biol.* **1998**, *8*, 799–809.

10.1021/jo900647d CCC: $40.75 © 2009 American Chemical Society
Published on Web 05/29/2009

port, and catalysis.[6] Recently, helical aromatic oligoamides[7] have attracted increasing interest for they feature a remarkable combination of structural predictability, stability, tunability, and ease of synthesis. Consequently, helical foldamers based on oligoanthranilamides,[8] oligopyridine dicarboxamides,[9] quinoline-derived oligoamides,[10] and meta-connected diaryl amides[11] have been developed. Moreover, previous theoretical and experimental studies demonstrated that variations in macromolecular architecture have an impact on the physical and chemical properties of foldamers in solution,[12] and structural changes of aromatic oligoamides induced by ion binding[13] and protonation[14,17b] have been described. However, there are only a few studies directly evaluating the effect of localized shifts in the conformational equilibria of a structural subunit on the consequent global properties in solid and solution[15] induced by solvent[16] and temperature effects, and the examples are especially rare in aromatic oligoamides.

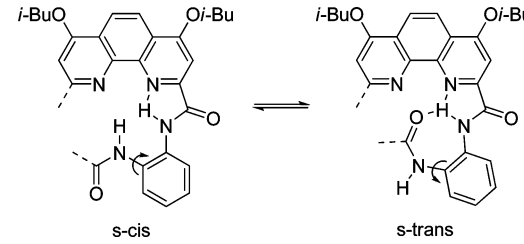

FIGURE 1. Local variation of steric interaction related to the amide s-cis/s-trans isomerization process in oligo(phenanthroline dicarboxamide)s.

We recently reported a new class of aromatic oligoamides based on phenanthroline dicarboxamides, which exhibited well-defined helical secondary structures in solution and in the solid state.[17] Furthermore, we presented the first artificial aromatic oligoamide based helix-turn-helix (HTH) supersecondary structure,[17b] and very recently, we demonstrated the helical molecular strands derived from the oligo(phenanthroline dicarboxamide)s displayed an acid- and base-controlled structural switching process,[17c] and also found such helical foldamers could be applied in folding-induced selective reduction of the 9,10-anthraquinone analogues.[17d] As part of our continuing work, we herein experimentally and theoretically characterize the structural features of the oligo(phenanthroline dicarboxamide)s and their dynamic environment-associated conformational conversion from secondary to supersecondary structure, owing to the conversion of the CONH−aryl bond from s-cis form to s-trans form.

Results and Discussion

Design Principles. It is difficult to predict the conformation of a macromolecule or supramolecule; however, a major structural change of macromolecules or supramolecules sometimes depends on the conformational switching of a small structural unit.[18] Therefore, there has been considerable interest in understanding, predicting, and controlling the conformation of small structural units in the past few years.[19]

The *o*-phenylenediamide is an important structural unit in the backbone of oligo(phenanthroline dicarboxamide)s. Since there is no specific attractive or repulsive interaction between the two amides of the *o*-phenylenediamide moieties, it can form s-cis and s-trans conformations with rotation about the CONH−aryl bond (Figure 1), which can be a rate-limiting step in the folding mechanism. The factors that favor specific isomer geometry around *o*-phenylenediamide can thus contribute significantly toward controlling the structures of the oligo(phenanthroline

(4) (a) Hecht, S. M.; Huc, I. *Foldamers: Structure, Properties and Applications*; Wiley-VCH: Weinheim, Germany, 2007. (b) Gellman, S. H. *Acc. Chem. Res.* **1998**, *31*, 173–180. (c) Hill, D. J.; Prince, R. B.; Hughes, T. S.; Moore, J. S. *Chem. Rev.* **2001**, *101*, 3893–4011. (d) Cheng, R. P.; Gellman, S. H.; Degrado, W. F. *Chem. Rev.* **2001**, *101*, 3219–3232. (e) Seebach, D.; Hook, D. F.; Glattli, A. *Biopolymers* **2006**, *84*, 23–37.

(5) For some helical synthetic examples, see:(a) Seebach, D.; Overhand, M.; Kuehnle, F. N. M.; Martinoni, B.; Oberer, L.; Hommel, U.; Widmer, H. *Helv. Chim. Acta* **1996**, *79*, 913–941. (b) Nelson, J. C.; Saven, J. G.; Moore, J. S.; Wolynes, P. G. *Science* **1997**, *277*, 1793–1796. (c) Appella, D. H.; Christianson, L. A.; Klein, D. A.; Richards, M. A.; Powell, D. R.; Gellman, S. H. *J. Am. Chem. Soc.* **1999**, *121*, 7574–7581. (d) van Gorp, J. J.; Vekemans, J. A. J. M.; Meijer, E. W. *Chem. Commun.* **2004**, 60–61. (e) Claridge, T. D. W.; Long, D. D.; Baker, C. M.; Odell, B.; Grant, G. H.; Edwards, A. A.; Tranter, G. E.; Fleet, G. W. J.; Smith, M. D. *J. Org. Chem.* **2005**, *70*, 2082–2090. (f) Violette, A.; Averlant-Petit, M. C.; Semetey, V.; Hemmerlin, C.; Casimir, R.; Graff, R.; Marraud, M.; Briand, J.-P.; Rognan, D.; Guichard, G. *J. Am. Chem. Soc.* **2005**, *127*, 2156–2164. (g) Menegazzo, I.; Fries, A.; Mammi, S.; Galeazzi, R.; Martelli, G.; Orena, M.; Rinaldi, S. *Chem. Commun.* **2006**, 4915–4917. (h) Goto, H.; Katagiri, H.; Furusho, Y.; Yashima, E. *J. Am. Chem. Soc.* **2006**, *128*, 7176–7178. (i) Vasudev, P. G.; Ananda, K.; Chatterjee, S.; Aravinda, S.; Shamala, N.; Balaram, P. *J. Am. Chem. Soc.* **2007**, *129*, 4039–4048. (j) Ousaka, N.; Sato, T.; Kuruda, R. *J. Am. Chem. Soc.* **2008**, *130*, 463–365. (k) Baruah, P. K.; Gonnade, R.; Rajamohanan, P. R.; Hofmann, H.-J.; Sanjayan, G. J. *J. Org. Chem.* **2007**, *72*, 5077–5084.

(6) (a) Estroff, L. A.; Incarvito, C. D.; Hamilton, A. D. *J. Am. Chem. Soc.* **2004**, *126*, 2–3. (b) Cornelissen, J. J. L. M.; Donners, J. J. J. M.; de Gelder, R.; Graswinckel, W. S.; Metselaar, G. A.; Rowan, A. E.; Sommerdijk, N. A. J. M.; Nolte, R. J. M. *Science* **2001**, *293*, 676–680.

(7) (a) Huc, I. *Eur. J. Org. Chem.* **2004**, *1*, 17–29. (b) Gong, B. *Acc. Chem. Res.* **2008**, *41*, 1376–1386. (c) Li, Z.-T.; Hou, J.-H.; Li, C. *Acc. Chem. Res.* **2008**, *41*, 1343–1353.

(8) (a) Hamuro, Y.; Geib, S. J.; Hamilton, A. D. *Angew. Chem., Int. Ed. Engl.* **1994**, *33*, 446–448. (b) Hamuro, Y.; Geib, S. J.; Hamilton, A. D. *J. Am. Chem. Soc.* **1996**, *118*, 7529–7541. (c) Hamuro, Y.; Hamilton, A. D. *Bioorg. Med. Chem.* **2001**, *9*, 2355–2363.

(9) (a) Berl, V.; Huc, I.; Khoury, R. G.; Krische, M. J.; Lehn, J.-M. *Nature* **2000**, *407*, 720–723. (b) Haldar, D.; Jiang, H.; Léger, J.-M.; Huc, I. *Angew. Chem., Int. Ed.* **2006**, *45*, 5483–5486. (c) Zhan, C.; Léger, J.-M.; Huc, I. *Angew. Chem., Int. Ed.* **2006**, *45*, 4625–4628.

(10) (a) Jiang, H.; Léger, J.-M.; Huc, I. *J. Am. Chem. Soc.* **2003**, *125*, 3448–3449. (b) Gillies, E. R.; Deiss, F.; Staedel, C.; Schmitter, J. M.; Huc, I. *Angew. Chem., Int. Ed.* **2007**, *46*, 4081–4084. (c) Dolain, C.; Jiang, H.; Léger, J.-M.; Guionneau, P.; Huc, I. *J. Am. Chem. Soc.* **2005**, *127*, 12943–12951. (d) Gillies, E. R.; Dolain, C.; Léger, J.-M.; Huc, I. *J. Org. Chem.* **2006**, *71*, 7931–7939. (e) Gan, Q.; Bao, C.; Kauffmann, B.; Grélard, A.; Xiang, J.; Liu, S.; Huc, I.; Jiang, H. *Angew. Chem., Int. Ed.* **2008**, *47*, 1715–1718.

(11) (a) Yuan, L. H.; Zeng, H. Q.; Yamato, K.; Sanford, A. R.; Feng, W.; Atreya, H. S.; Sukumaran, D. K.; Szyperski, T.; Gong, B. *J. Am. Chem. Soc.* **2004**, *126*, 16528–16537. (b) Yuan, L. H.; Sanford, A. R.; Feng, W.; Zhang, A. M.; Zhu, J.; Zeng, H. Q.; Li, M. F.; Ferguson, J. S.; Gong, B. *J. Org. Chem.* **2005**, *70*, 10660–10669. (c) Sanford, A. R.; Gong, B. *Curr. Org. Chem.* **2003**, *7*, 1649–1659.

(12) (a) Balzani, V.; Credi, A.; Venturi, M. *Molecular Devices and Machines*; Wiley-VCH: Weinheim, Germany, 2004. (b) de Silva, A. P.; McClenaghan, N. D. *Chem.—Eur. J.* **2004**, *10*, 574–586. (c) Irie, M. *Chem. Rev.* **2000**, *100*, 1685–1716.

(13) (a) Barboiu, M.; Lehn, J.-M. *Proc. Natl. Acad. Sci. U.S.A.* **2002**, *99*, 5201–5206. (b) Stadler, A. M.; Kyritsakas, N.; Lehn, J.-M. *Chem. Commun.* **2004**, 2024–2025.

(14) (a) Dolain, C.; Maurizot, V.; Huc, I. *Angew. Chem., Int. Ed.* **2003**, *42*, 2738–2740. (b) Kolomiets, E.; Berl, V.; Odriozola, I.; Stadler, A. M.; Kyritsakas, N.; Lehn, J.-M. *Chem. Commun.* **2003**, 2868–2869. (c) Kolomiets, E.; Berl, V.; Lehn, J.-M. *Chem.—Eur. J.* **2007**, *13*, 5466–5479.

(15) (a) Lockman, J. W.; Paul, N. M.; Parquette, J. R. *Prog. Polym. Sci.* **2005**, *30*, 423–452. (b) Hamuro, Y.; Geib, S. J.; Hamilton, A. D. *J. Am. Chem. Soc.* **1996**, *118*, 7529–7541.

(16) For examples for structural changes of oligomers induced solvent effects, see. (a) Hill, D. H.; Moore, J. S. *Proc. Natl. Acad. Sci. U.S.A.* **2002**, *99*, 5053–5057. (b) Zhao, Y.; Zhong, Z. *J. Am. Chem. Soc.* **2005**, *127*, 17894–17901.

(17) (a) Hu, Z.-Q.; Hu, H.-Y.; Chen, C.-F. *J. Org. Chem.* **2006**, *71*, 1131–1138. (b) Hu, H.-Y.; Xiang, J.-F.; Yang, Y.; Chen, C.-F. *Org. Lett.* **2008**, *10*, 69–72. (c) Hu, H.-Y.; Xiang, J.-F.; Yang, Y.; Chen, C.-F. *Org. Lett.* **2008**, *10*, 1275–1278. (d) Hu, H.-Y.; Xiang, J.-F.; Cao, J.; Chen, C.-F. *Org. Lett.* **2008**, *10*, 5035–5038.

(18) (a) Clayden, J.; Lund, A.; Vallverdú, L.; Helliwell, M. *Nature* **2004**, *431*, 966–971. (b) Kern, D.; Zuiderweg, E. R. P. *Curr. Opin. Struct. Biol.* **2003**, *13*, 748–757. (c) Seebach, D.; Schreiber, J. V.; Abele, S.; Daura, X.; van Gunsteren, W. F. *Helv. Chim. Acta* **2000**, *83*, 34–57.

(19) Okamoto, I.; Nabeta, M.; Hayakawa, Y.; Morita, N.; Takeya, T.; Masu, H.; Azumaya, I.; Tamura, O. *J. Am. Chem. Soc.* **2007**, *129*, 1892–1893.

dicarboxamide)s. However, in our preceding research, the *o*-phenylenediamide bonds all favored s-cis conformation, which made the oligomers form secondary helical structures in solid and solution.[17] Subsequently, we wonder whether the helical structure is the only conformation of these oligo(phenanthroline dicarboxamide)s, and whether the conformation of *o*-phenylenediamide bonds could change to the s-trans conformation in response to environmental factors such as solvent acceptor ability. To confirm this thought, we decided to choose the oligomers with three phenanthroline units as the model for investigating the conformational conversion phenomena. When the conformational transition occurs in one of the *o*-phenylenediamide subunits in the oligomer triggered by an s-cis to s-trans 180° rotation, the simplest environment-associated supersecondary helix-turn structure will be formed.

Solid-State Structure of Oligomer 3a. Understanding the fundamental principles of protein folding requires the integration of experimental and theoretical approaches. X-ray crystallography is the preeminent technique in the determination of protein structure. In the oligo(phenanthroline dicarboxamide)s, the special conversion phenomenon was first observed in the X-ray single-crystal structure of oligomer **3a**, which also provided direct evidence for the formation of the helix-turn supersecondary structure. The single crystals of oligomer **3a** suitable for X-ray diffraction were obtained from its mixture solution of CH_2Cl_2/MeOH through slow evaporation at room temperature. As shown in Figure 2b, the oligomer **3a** consisted of a regular helix and a turn, which formed a helix-turn supersecondary motif. It was found that the helical pitch in **3a** is about 3.5 Å, which indicates intramolecular $\pi-\pi$ stacking between the two phenanthroline. In addition, the turn side was also stabilized by an additional intramolecular seven-membered hydrogen bond between the amides with a C═O···HN distance of 2.49 Å. Interestingly, we further found that one MeOH molecule was presented at the outside of one of the helical terminals (Figure 2c). There exist multiple intermolecular hydrogen bonds between the methanol molecule and the helix, which enhanced the helical stability. It is also noteworthy that after the inversion, there is an intermolecular face-to-face $\pi-\pi$ stacking between the two phenanthroline rings of the adjacent foldamers with a distance of 3.50 Å, which can bring about significant additional stabilization of the supersecondary structure.

We attempted to grow the single crystals of **3a** from other solutions and hoped to obtain the regular helical structure. As a result, the oligomer **3a** similarly crystallized from CH_2Cl_2/CH_3CN, affording a clear, triclinic crystal with a $P\bar{1}$ space group; however, the X-ray experiment result showed that **3a** still forms the helix-turn structure, and there was a H_2O molecule instead of MeOH at each end of the helix-turn (Figure 2d). The turn side was also stabilized by an additional intramolecular seven-membered hydrogen bond between the amides with a C═O···HN distance of 2.45 Å. The intermolecular distance between the two planes containing the phenanthroline groups is 3.50 Å, corresponding to the van der Waals contact. We considered that because of the addition of intermolecular face-to-face $\pi-\pi$ stacking at the turn side, the helix-turn structure is more stable than the helix structure in the crystal state. Since crystallization is a kinetically controlled process, this X-ray structure does not necessarily represent the energy minimum of the system.

Solution-State Structure. Variable-temperature ^{1}H NMR studies on oligomer **1a**−**4a** were further carried out to examine their conformations in $CDCl_3$ solution. At 213 K and a

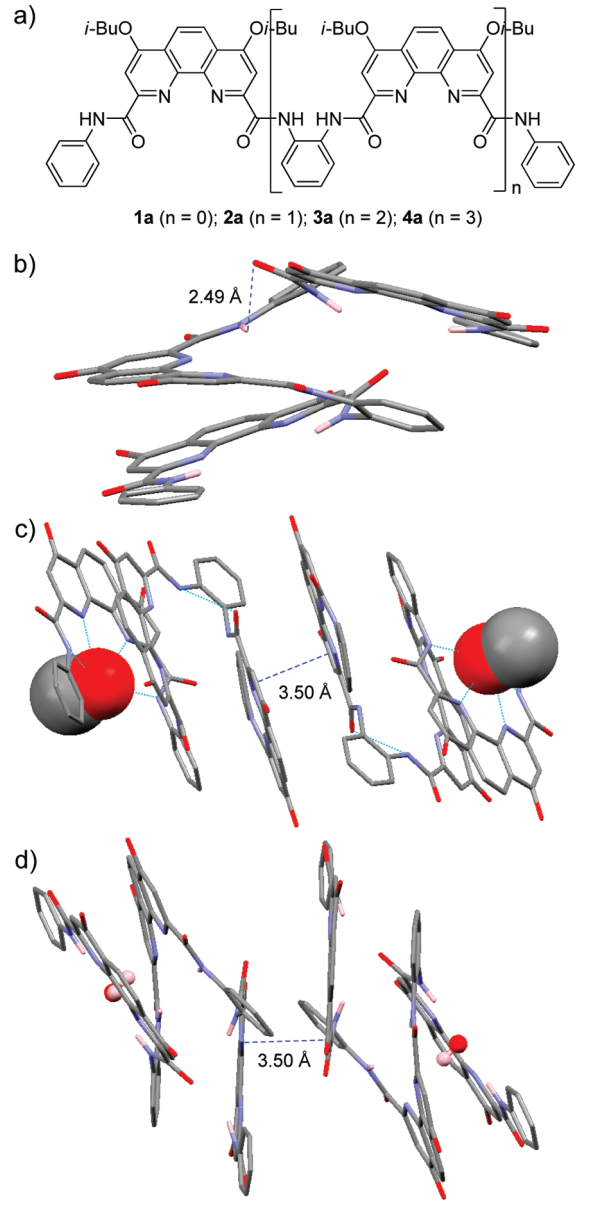

FIGURE 2. (a) Chemical structures of oligomers**1a**−**4a**. (b) Crystal structures of **3a** obtained in CH_2Cl_2/CH_3OH. (c) Crystal packing of **3a** with methanol molecules presented at the helical ends. (d) Crystal packing of **3a** with H_2O molecules presented at the helical ends obtained in CH_2Cl_2/CH_3CN. Isobutyl chains and hydrogen atoms not involved in the hydrogen bonds are omitted for clarity.

concentration of 10 mM, no new signals were observed for oligomers **1a** and **2a**, which indicated oligomers **1a** and **2a** preferred stable planar and helical conformations, respectively (see the Supporting Information). In contrast, the ^{1}H NMR spectra of oligomers **3a** and **4a** exhibited more sensitivity to temperature. As shown in Figure 3, **3a** shows the spectrum of a compound of *C*2 symmetry at room temperature (298 K), which suggests that the inversion between different conformations is fast in the NMR time scale. With lowering of the temperature, signals corresponding to NHs broadened. At 238 K, new signals in the NH zone appeared, while new broad signals also came into sight in the area between 6 and 9 ppm. These observations implied that more than one conformation of the oligomer in solution could exist at low temperature and the interconverting equilibrium of the two conformations (s-cis and s-trans) might depend on temperature. For the longer

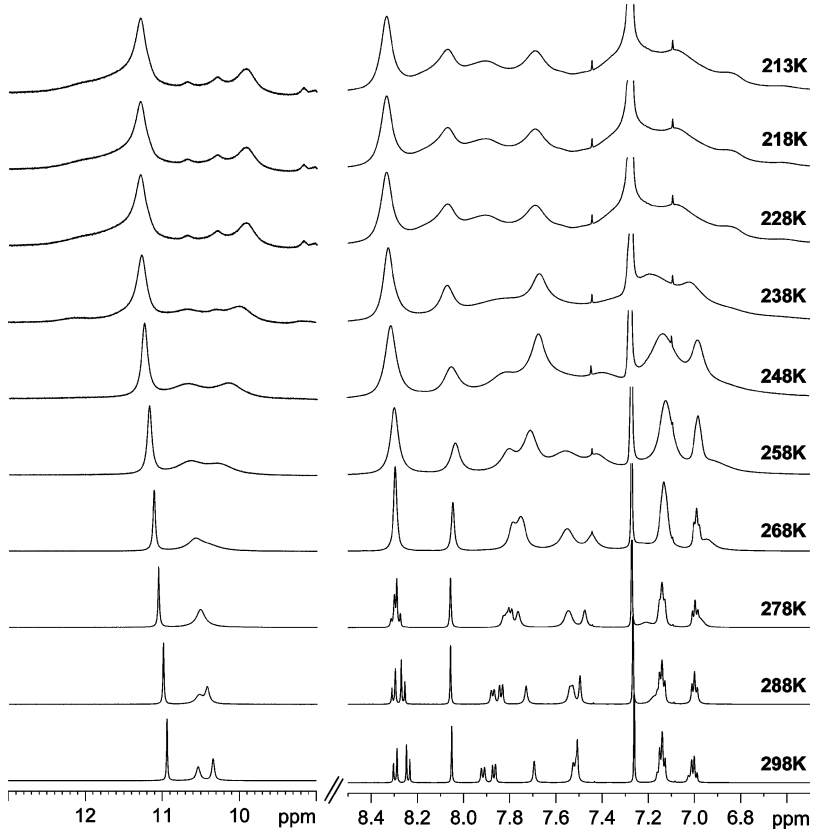

FIGURE 3. Temperature-dependent ^{1}H NMR spectra (600 MHz, 10 mM, $CDCl_3$) of **3a**.

oligomer **4a** at the same condition, two sets of signals for *C*2 symmetrical molecules were observed at 213 K. The NHs signals, which appeared broad in the downfield area between 9.9 and 11.3 ppm at 298 K, exhibited 8 sharp signals in this field (see the Supporting Information). This indicated that the NH bonds of the middle *o*-phenylenediamides might invert from s-cis form to s-trans form, and the oligomer **4a** could adopt both secondary and supersecondary conformations at low temperature.

Chirality Induction. Circular dichroism (CD) spectroscopy is of considerable importance to the study of proteins as a quantitative tool in the estimation of secondary structure,[20] and it is also a useful tool to investigate the secondary structure of synthetic oligomers.[21] Therefore, to investigate the conformational properties of the oligomers in solution, a chiral, nonracemic 1-phenylethanamine group was employed as the terminal to cause the *M* and *P* helical conformations at the periphery to be related as diastereomeric conformations, and the effect of solvent on the special conformational preference of the oligomers could be investigated by CD spectroscopy.[22] First, we used oligomers **1**−**4** to carry out their CD experiments in methanol at room temperature. As shown in Figure 4, the helical foldamers **2**−**4** show a positive and then a negative CD band between 300 and 420 nm due to the $\pi-\pi^*$ electronic transition of the phenanthroline moiety, which indicates that the oligoamides may have a predominant one-handed (*R*-*M*) helical structure.[23]

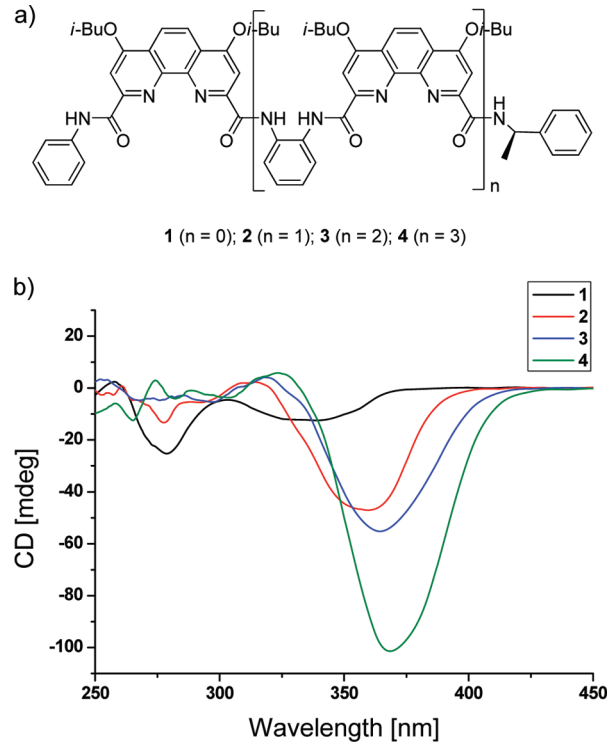

FIGURE 4. (a) Chemical structures of oligomers **1**−**4** and (b) CD spectra of oligomers **1**−**4** in MeOH ($c = 5 \times 10^{-5}$ M).

However, in contrast with the amplification of the optical activity CD spectra of helical oligomers **1**−**4** in acetonitrile,[17c] the intensity of the molar CD ($\Delta\varepsilon$) of **2** and **3** is almost the same in methanol. There is a loss of helicity in longer oligomer **3**, in

(20) Whitford, D. *Protions Structure and Function*; John Wiley & Sons, Ltd.: Chichester, England, 2006.
(21) (a) *Circular Dichroism and the Conformational Analysis of Biopolymers*; Fasman, G. D., Ed.; Plenum Publishing: New York, 1996. (b) Maeda, K; Yashima, E. *Top. Curr. Chem.* **2006**, *265*, 47–88.
(22) (a) Parquette, J. R. *C. R. Chimie* **2003**, *6*, 779–789. (b) Hofacker, A. L.; Parquette, J. R. *Angew. Chem., Int. Ed.* **2005**, *44*, 1053–1057.

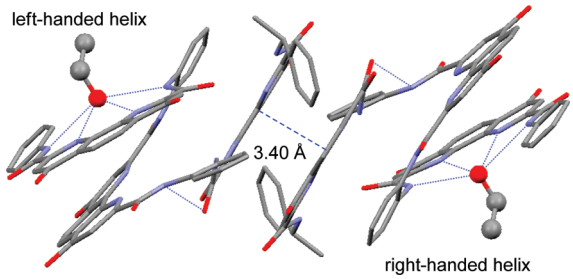

FIGURE 5. Crystal structure of **3** with ethanol molecules presented at the helical ends. Isobutyl chains and hydrogen atoms not involved in the hydrogen bonds are omitted for clarity.

agreement with our assumption that besides the helical structure, strand **3** may have the other conformations in methanol. Next, the temperature dependence of the oligo(phenanthroline dicarboxamide)s on their conformational conversion behavior was also investigated by CD spectroscopy in acetonitrile and in methanol. In contrast to oligomer **2**, which displayed preferences for the helical conformation in both the acetonitrile and methanol solvents, oligomers **3** and **4** were significantly affected by external conditions, such as the solvent and temperature. The molar CD values at 363 nm of oligomers **3** and **4** in acetonitrile slightly increased, which demonstrated that their helical conformations were more stable in acetonitrile with decreasing temperature. However, decreasing the temperature of a solution of oligomers **3** and **4** in methanol from 25 to −10 °C led to destabilization of the helical conformation as evidenced by the decreasing CD intensity at 363 nm (see the Supporting Information). To obtain more insights into the effect of solvent on the special conformation, we further carried out the CD experiments of oligomers **1**−**4** in CH_2Cl_2 and high-polarity solvent DMSO (see the Supporting Information). Similar bandshapes were obtained in each of the solvents, and the $\Delta\varepsilon$ values increased as the numbers of the phenanthroline group increased in both of the solvents, which indicated that the helical structures are more stable. These studies support the supposition that the solution is a source of or contributing factor to the s-cis and s-trans conformation inversion. In nonprotic solutions, a highly biased helical secondary structure is present in **3**, and it is guided to secondary and helix-turn supersecondary conformation equilibria in protic solutions.

A clear, colorless plate-like crystal of oligomer **3** was obtained by slow evaporation of an EtOH solution. The crystal structure indicated that the oligomer adopts a helical-turn conformation in the solid state (Figure 5). Similar to oligomer **3a**, there is also an intermolecular $\pi-\pi$ stacking at the turn side. It is noteworthy that, because of the inversion, both the right-handed and the left-handed diastereomers have cocrystallized in the crystal structures, which could give any CD singles in the phenanthroline UV-absorbing region at 363 nm. That may be one reason that the intensities of the molar CD ($\Delta\varepsilon$) of **2** and **3** are almost the same in methanol.

The fluxional nature of the molecule was evident in the temperature-dependent ^{1}H NMR spectra of **3** in $CDCl_3$ (Figure 6). At room temperature (298 K), only one set of signals of oligomer **3** were observed, which indicated an extremely biased conformational equilibrium or the inversion between different conformations was fast in the NMR time scale. With lowering of the temperature, signals corresponding to NHs and the aromatic protons broadened. At a temperature where the rate of conformation interconversion was slow on the NMR time scale, new signals in the NH zone appeared; new broad signals also come into sight in the area between 6 and 9 ppm, which

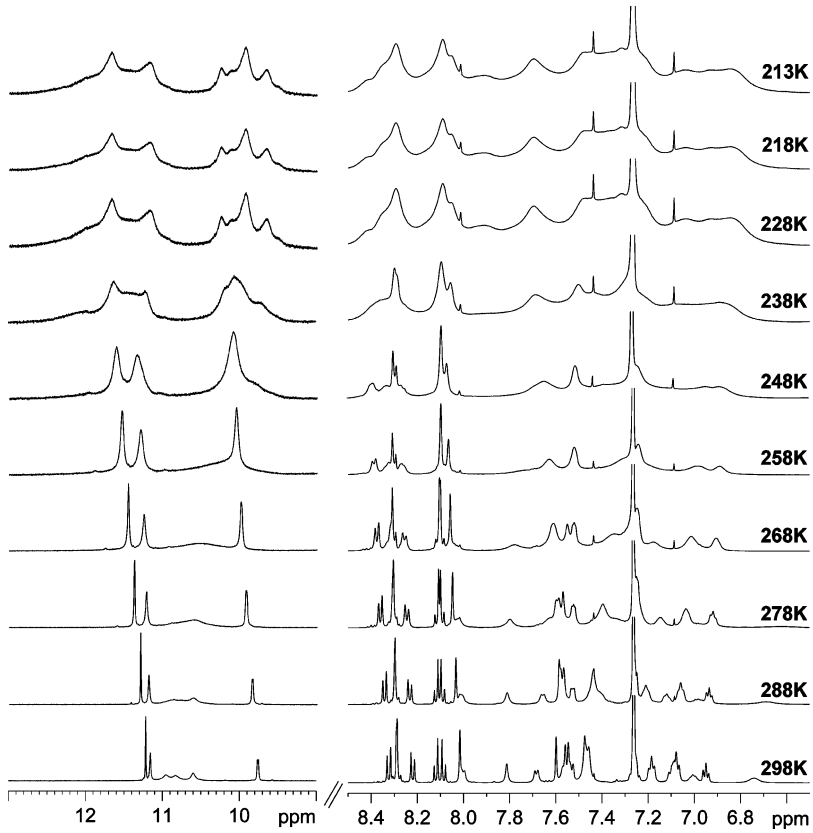

FIGURE 6. Temperature-dependent ^{1}H NMR spectra (600 MHz, 10 mM, $CDCl_3$) of **3**.

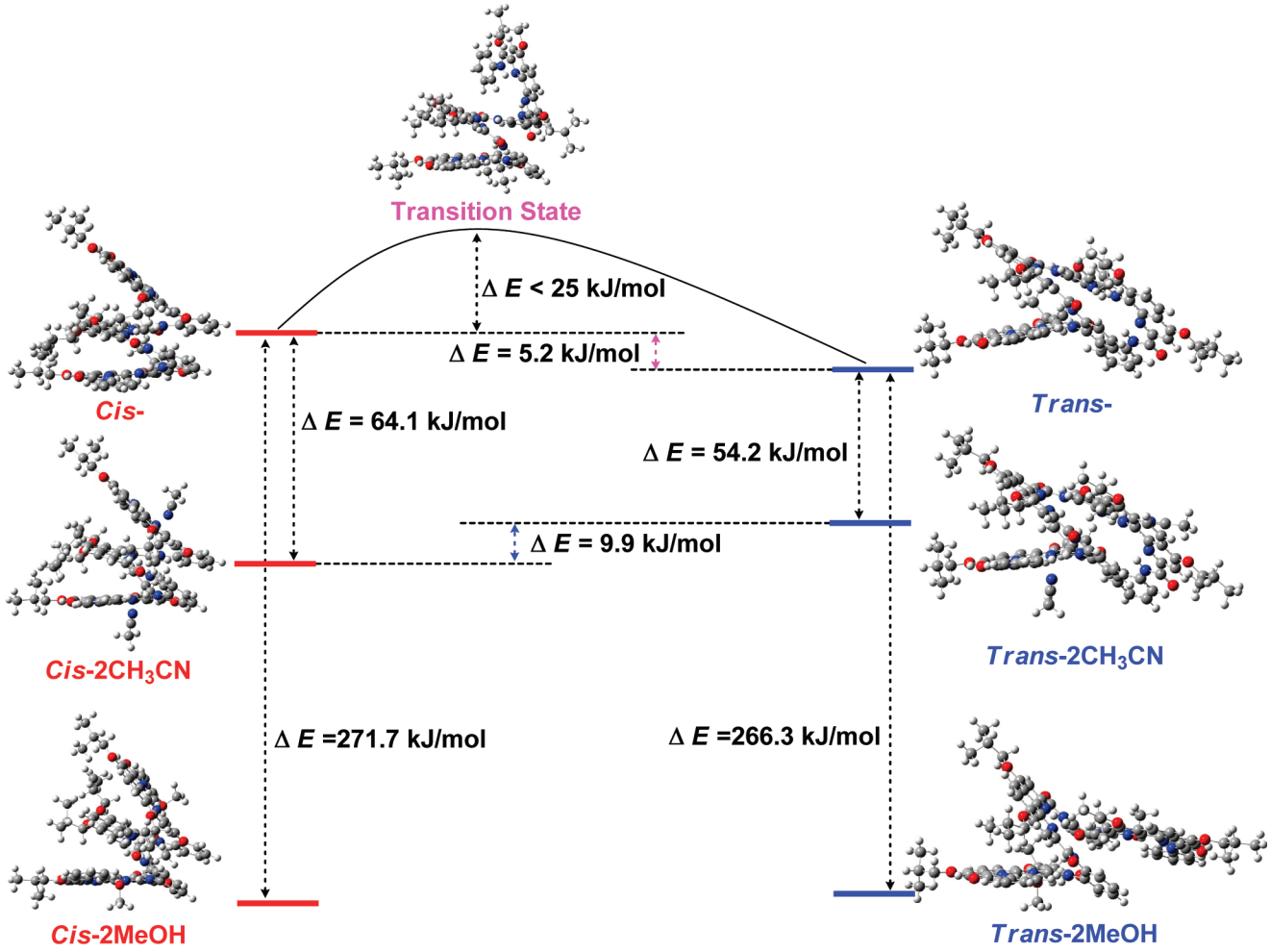

FIGURE 7. Optimization of oligo(phenanthroline dicarboxamide) **3a** at the B3LYP/3-21g** level.

indicated another conformation of oligomer **3** appeared. We also take the variable-temperature ^{1}H NMR studies on the longer strand **4**. Similar to **4a**, multiple sets of sharp signals were observed at 213 K; however, it is hard for us to confirm the position of the NH bonds of the *o*-phenylenediamides which inverted from s-cis form to s-trans form (see the Supporting Information).

Conformational Energy and Molecular Dynamics Simulations of Oligomer 3a. Computational studies suggest the possibility of conformational conversion from secondary to supersecondary structure. We calculated the difference in free energy (ΔG) between the helically ordered state and the supersecondary helix-turn conformations of oligomer **3a**. Optimization of oligo(phenanthroline dicarboxamide) **3a** at the B3LYP/3-21g** level of theory revealed two unique conformations. These conformations corresponded to carboxamide groups of the *o*-phenylenediamide toward the same direction or opposite directions, one s-cis conformer and s-trans conformer. In the gas phase (Figure 7), the helix-turn conformer is the most stable. The second lowest energy conformer was the helical structure. They differ from the former by an ca. 180° rotation about one of the aryl-−H linkages on one of the *o*-phenylenediamide rings, which can occur with disruption of one intramolecular hydrogen bond but addition of $\pi-\pi$ stacking. These rotations result in an over 5.2 kJ/mol additional conformational energy. The energy barrier for rotation is only 25 kJ/mol. To simplify the research model, we added two solvent molecules instead of the solvent. It is noteworthy that the preference for s-trans over s-cis conformations decreases significantly from 5.2 kJ/mol in the gas phase to −9.9 kJ/mol in **3a**-2CH_3CN, which means that the helical structure is much more stable than the helix-turn structure in CH_3CN. It is also worthy of note that the preference for s-cis conformation becomes very small (about 0.1 kJ/mol) when two MeOH molecules are added to oligomer **3a**. In this case, the helical structure and the helix-turn structure will both exist in MeOH. Accordingly, we can conclude that together with hydrogen bonds and intramolecular $\pi-\pi$ stacking, solvent effects also play an important role in the stability of oligo(phenanthroline dicarboxamide)s. Theoretical conformational searching of **3a** with the B3LYP/3-21g** predicts a helical structure in nonprotic solvent whereas it predicts a conformational equilibria of helical and helix-turn structures in protic solvent, in accord with the CD studies. It also demonstrated that the low energy barrier to the s-cis/s-trans interconvertion produced a highly dynamic conformational equilibrium at ambient temperature. This work suggests the potential of foldamers to exhibit conformational responses to localized structural perturbations.

(23) Tanatani, A.; Yokoyama, A.; Azumaya, I.; Takakura, Y.; Mitsui, C.; Shiro, M.; Uchiyama, M.; Muranaka, A.; Kobayashi, N.; Yokozawa, T. *J. Am. Chem. Soc.* **2005**, *127*, 8553–8561.

SCHEME 1. Synthetic Route of Compounds 5−7

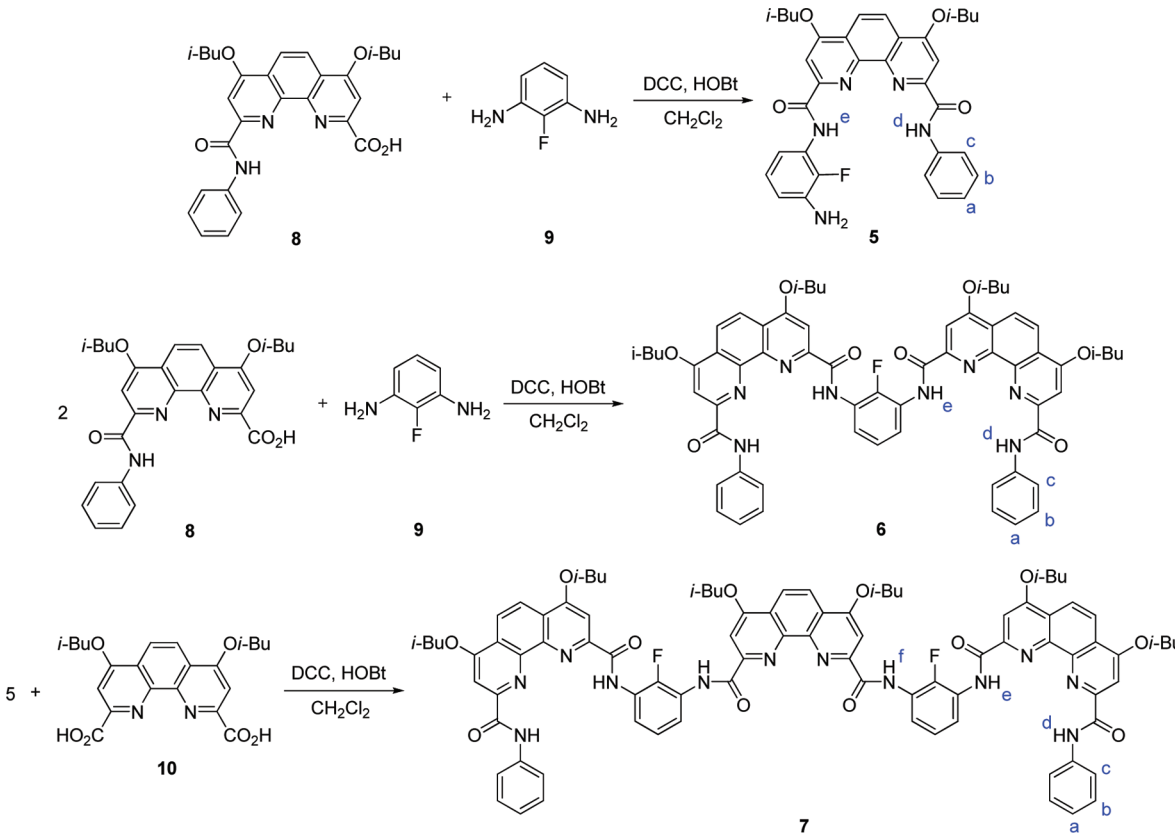

Restricted Rotation Around the CONH−Aryl Bonds. Rotation around the CONH−aryl bonds could be restricted by a hydrogen bond between the amide proton and a hydrogen bond acceptor at the ortho position on the aryl group.[7a] In ref 24, the intramolecular F···H−N hydrogen bond has been utilized to stabilize the binding conformation of the oligomers; therefore, the fluorine-containing compounds **5**−**7** were synthesized, which were prepared from the appropriate acid with 2-fluorobenzene-1,3-diamine[25] in dichloromethane in the presence of dicyclohexylcarbodiimide and 1-hydroxybenzotriazole (Scheme 1). Compounds **5**−**7** have been characterized by ^{1}H NMR, ^{13}C NMR, elemental analyses, and MALDI-TOF mass spectrometry.

Figure 8 shows the ^{1}H NMR spectra of solutions of **5**−**7** in $CDCl_3$. Increasing strand length results in a strong shielding of aromatic protons H_a, H_b, and H_c, which can be attributed to tight contacts between aromatic rings. The ^{1}H NMR spectra are consistent with helical structures of **6** and **7**, which have been assigned stacked, possibly helical conformations in solution.

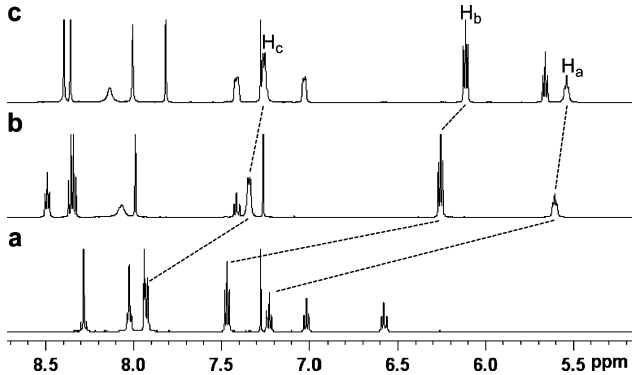

FIGURE 8. Partial ^{1}H NMR spectra (10 mM, 600 MHz, $CDCl_3$, 283K) of (a) **5**, (b) **6**, and (c) **7**.

The X-ray crystal structures of **6** and **7** have been determined, and they showed that both molecules take up a helical conformation in the solid state. The structure of **6** shows (Figure 9a,b) a clear helical arrangement of the five rings stabilized by a network of intramolecular hydrogen bonds (NH_e···N, 2.05 Å; NH_e···F, 2.30 Å; NH_d···N, 2.19 Å). Figure 9b shows the left-handed helix with a complete turn; however, the crystal is racemic with both right- and left-handed forms present in the unit cell. The structure of the longer strand **7** also shows (Figure 9c,d) a clear helical arrangement of the five rings stabilized by a network of intramolecular hydrogen bonds (NH_f···N, 2.11 Å; NH_e···F, 2.28 Å; NH_e···N, 2.06 Å; NH_e···F, 2.21 Å; NH_d···N, 2.23 Å). This network of hydrogen bonds serves to restrict the rotation about the CONH−aryl bonds to a cisoid conformation, and the oligomer assumes an overall helix shape. Similar to oligomer **6**, Figure 9d shows the right-handed helix with two turns; however, the crystal is also racemic with both right- and left-handed forms present in the unit cell. Accordingly, we can conclude that the addition of the F···H−N hydrogen bond could be utilized to stabilize the binding conformation of the oligomers. The F···H−N distance is between 2.30 and 2.21 Å, which is about 15% shorter than the sun of the van der Waals radii (2.67 Å). Compared with the crystal structures of the *o*-phenylenediamide connecting oligomers reported by us before, the increase in the hole of the helix made the partial overlap of the two adjacent phenanthroline units disappeared, which reduced the $\pi-\pi$ stacking of the oligomers, hence, the F···H−N

(24) Li, C.; Ren, S.-F.; Hou, J.-L.; Yi, H.-P.; Zhu, S.-Z.; Jiang, X.-K.; Li, Z.-T. *Angew. Chem., Int. Ed.* **2005**, *44*, 5725–5729.
(25) Hudilicky, M.; Bell, H. M. *J. Fluorine Chem.* **1974**, *4*, 19–23.

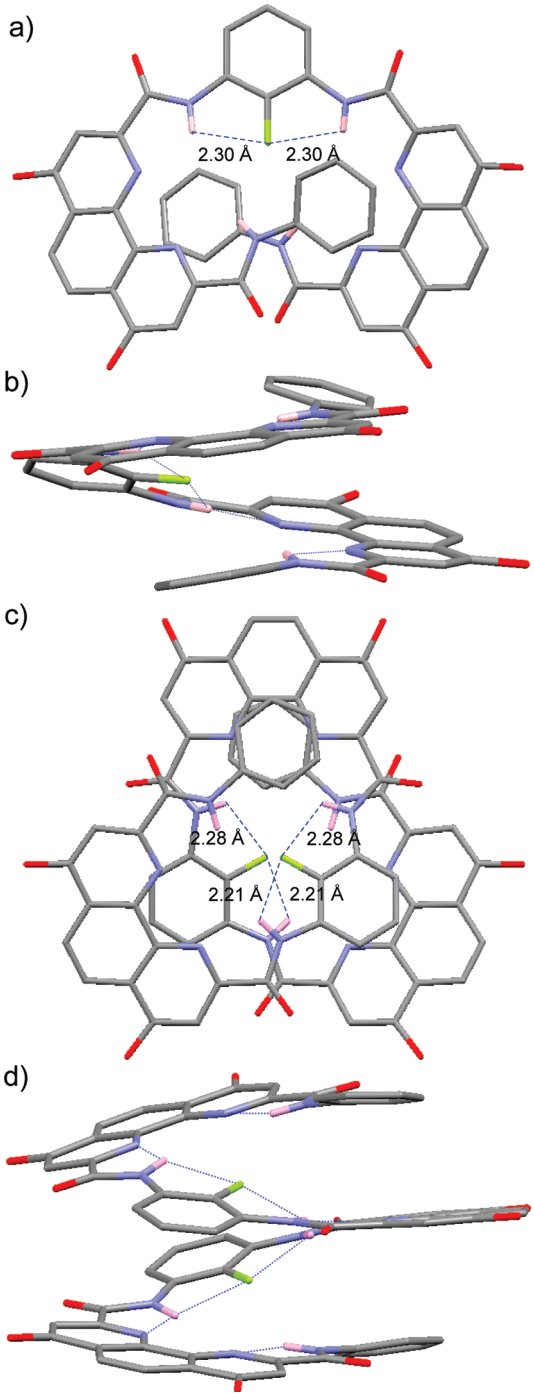

FIGURE 9. Crystal structures of the (a) top view and (b) side view of **6** and the (c) top view and (d) side view of **7**. Isobutyl chains and hydrogen atoms not involved in the hydrogen bonds are omitted for clarity.

hydrogen bond plays a key role in the enhanced helical stability. This simple expansion of the helical structure offers potential in the future for subtle modification of the folded structures.

Conclusion

In conclusion, we have characterized the structural features of the oligo(phenanthroline dicarboxamide)s, and presented their dynamic environment-associated conformational conversion from secondary helical structures to supersecondary helix-turn structures by X-ray crystallographic, variable-temperature ^{1}H NMR, variable-temperature circular dichroism techniques, and computational studies. We have further demonstrated that the solvent effects together with intramolecular hydrogen bonds and $\pi-\pi$ stacking play a key role in stabilizing both the secondary and supersecondary structures. Moreover, we have also proved that by introducing the intramolecular F···H−N hydrogen bond to restrict the rotation about the CONH−aryl bonds, the oligomers **6** and **7** subsequently showed well-defined and predictable secondary helical conformations in solution and in the solid state. The results presented here suggested that similar to biomolecules, the differences in local conformational equilibria of the oligo(phenanthroline dicarboxamide)s could also be dominated by hydrophobic effects at the global structural level, and this environment-responsive type of conformational control could have considerable potential for controlling the shape of macromolecules or supramolecules. Our further work will focus on the investigation of the possible conformations of the longer and more complicated systems, and develop materials with novel functional capabilities exhibiting an amplified global environment response to a local event.

Experimental Section

Quantum Chemical Calculations. All quantum chemical calculations were performed at the B3LYP/3-21g** level of ab initio MO theory employing the Gaussian03 software package. The geometries of the molecules were completely optimized.

X-ray Crystallography. X-ray diffraction data for compounds **3a** obtained in CH_2Cl_2/CH_3OH, **3a** obtained in CH_2Cl_2/CH_3CN, **3**, **6**, and **7** were collected on a Rigaku Saturn X-ray diffractometer with graphite-monochromator Mo Kα radiation ($\lambda = 0.71073$ Å). Intensities were collected for absorption effects by using the multiscan technique SADABS. The structures were solved by direction methods and refined by a full matrix least-squares technique based on F^2, using SHELXL 97 program. All non-hydrogen atoms were refined anisotropically and H atoms were located from difference electron density maps. Especially for **7**, the disordered solvent molecules were deleted with the SQUEEZE program. The crystals **6** and **7** were easy to effloresce, so they were all measured in sealed tubes. The poor qualities of the structures may be due to weak diffraction intensity and strong disorganization of isobutyl side chains and included solvent molecules. However, all C and N atoms belonging to the backbone of the helix except those for the end benzene rings were accurately located. The X-ray crystallographic data are summarized in Table 1.

Compound 5. To the solution of 2-fluorobenzene-1,3-diamine **9** (630 mg, 5 mmol) in CH_2Cl_2 (50 mL) were added the acid **8** (2.43 g, 5 mmol), 1-hydroxylbenzotriazole (HOBt) (1.24 mg, 6 mmol), and DCC (918 mg, 6 mmol). The reaction mixture was stirred at room temperature, and then refluxed for 10 h. The precipitates were removed by filtration through the Celite. The solution was concentrated, and the residue was washed with MeOH. The solid was purified by silica gel column chromatography (ethyl acetate/dichloromethane/petroleum ether 1:2:3) to give the product (yield 91%) as a white solid. Mp >300 °C; ^{1}H NMR ($CDCl_3$, 600 MHz) δ 11.12 (d, 1H, $J = 2.1$ Hz, N*H*), 10.44 (s, 1H, N*H*), 8.28 (d, 2H), 8.03 (t, 2H, $J = 7.5$ Hz), 7.94 (s, 1H), 7.93 (d, $J = 8.0$ Hz, 2H), 7.47 (t, $J = 7.7$ Hz, 2H), 7.23 (t, $J = 7.4$ Hz, 1H), 7.02 (t, $J = 7.9$ Hz, 1H), 6.58 (t, $J = 7.9$ Hz, 1H), 4.14 (d, 2H, $J = 6.5$ Hz, $-OCH_2CH(CH_3)_2$), 4.12 (d, 2H, $J = 6.5$ Hz, $-OCH_2CH(CH_3)_2$), 3.62 (br s, 2H, $-NH_2$), 2.35−2.30 (m, 2H, $-OCH_2CH(CH_3)_2$), 1.19−1.17 (m, $-OCH_2CH(CH_3)_2$, 12H); ^{13}C NMR ($CDCl_3$, 150 MHz) δ 163.5, 163.4, 162.5, 161.9, 150.9, 150.5, 144.6, 144.58, 144.49, 143.0, 141.4, 137.8, 134.2, 134.1, 128.8, 126.85, 126.80, 124.75, 124.70, 124.67, 122.7, 121.4, 121.4, 120.6, 120.5, 112.1, 110.0, 101.9, 101.3, 75.6, 75.5, 28.23, 28.21, 19.2; MALDI-TOF MS *m/z* 596.3 $[M + H]^+$. Anal. Calcd for

TABLE 1. X-ray Crystallographic Data

	3a·CH_3OH	**3a**·H_2O	**3**	**6**	**7**
empirical formula	$C_{90}H_{90}N_{12}O_{12}$·CH_3OH	$C_{90}H_{90}N_{12}O_{12}$·H_2O	$C_{92}H_{94}N_{12}O_{12}$·$2CH_3CH_2OH$	$C_{62}H_{61}FN_8O_8$·$5CH_2Cl_2$	$C_{102}H_{103}F_2N_{12}O_{12}$
M_r	1562.77	1548.69	1651.93	1489.82	1726.96
crystal size [mm^3]	0.42 × 0.39 × 0.12	0.42 × 0.39 × 0.12	0.20 × 0.18 × 0.14	0.26 × 0.18 × 0.16	0.26 × 0.18 × 0.16
crystal system space group	triclinic	triclinic	triclinic	monoclinic	monoclinic
a [Å]	13.471(3)	13.257(3)	13.387(2)	20.318(4)	14.1007(16)
b [Å]	17.872(4)	18.769(4)	17.522(2)	18.965(4)	35.769(4)
c [Å]	18.764(4)	19.131(4)	23.044(3)	18.194(4)	22.459(2)
α [deg]	103.82(3)	117.56(3)	111.151(9)	90(9)	90
β [deg]	91.95(3)	91.60(3)	96.563(11)	90.13(3)	118.483(3)
γ [deg]	110.35(3)	103.68(3)	103.945(9)	90(9)	90
V [$Å^3$]	4079.2(14)	4047.9(15)	4770.2(11)	7011(2)	9956.5(19)
d [g cm^{-3}]	1.272	1.163	1.150	1.411	1.152
Z	2	2	2	4	4
T [K]	293(2)	293(2)	113(2)	113(2)	113(2)
R_1, wR_2 [$I > 2\sigma(I)$]	0.1551, 0.1551	0.1666, 0.2907	0.1343, 0.4111	0.0632, 0.1733	0.0699, 0.1973
R_1, wR_2 (all data)	0.4040, 0.2312	0.3297, 0.3913	0.1603, 0.4329	0.0742, 0.1832	0.0846, 0.2117
quality of fit	1.008	1.192	1.585	1.126	1.053

$C_{34}H_{34}FN_5O_4$: C, 68.56; H, 5.75; N, 11.76. Found: C, 68.30; H, 5.79; N, 11.67.

Compound 6. To the solution of 2-fluorobenzene-1,3-diamine **9** (315 mg, 2.5 mmol) in CH_2Cl_2 (50 mL) were added the acid **8** (2.43 g, 5 mmol), HOBt (1.24 mg, 6 mmol), and DCC (918 mg, 6 mmol). The reaction mixture was stirred at room temperature, and then refluxed for 10 h. The precipitates were removed by filtration through the Celite. The solution was concentrated, and the residue was washed with MeOH. The solid was purified by silica gel column chromatography (ethyl acetate/dichloromethane/petroleum ether 1:2:3) to give the product (yield 82%) as a white solid. Mp 280−281 °C; ^{1}H NMR ($CDCl_3$, 600 MHz) *δ* 11.22 (s, 2H, N*H*), 10.22 (br s, 2H, N*H*), 8.28 (d, 2H), 8.49 (t, 2H, *J* = 7.8 Hz), 8.37−8.33 (m, 4H), 8.07 (br s, 2H), 7.99 (s, 2H), 7.41 (t, *J* = 8.2 Hz, 1H), 7.34 (d, 4H), 6.27−6.24 (m, 4H), 5.61 (t, *J* = 6.8 Hz, 2H), 4.24−4.21 (m, 8H, $-OCH_2CH(CH_3)_2$), 2.42−2.37 (m, 4H, $-OCH_2CH(CH_3)_2$), 1.24−1.21 (m, $-OCH_2CH(CH_3)_2$, 24H); ^{13}C NMR ($CDCl_3$, 150 MHz) *δ* 163.4, 163.0, 162.3, 161.9, 150.8, 149.8, 144.7, 144.0, 142.4, 137.6, 127.6, 126.7, 126.6, 125.5, 122.6, 122.6, 122.4, 120.8, 120.1, 118.9, 115.2, 101.8, 100.9, 75.6, 28.3, 19.3; MALDI-TOF MS *m*/*z* 1065.6 $[M + H]^+$. Anal. Calcd for $C_{62}H_{61}FN_8O_8$·$0.5H_2O$: C, 69.32; H, 5.82; N, 10.43. Found: C, 69.25; H, 5.84; N, 10.44.

Compound 7. To the solution of **5** (1.19 mg, 2 mmol) in CH_2Cl_2 (50 mL) were added the acid **10** (412 mg, 1 mmol), HOBt (618 mg, 3 mmol), and DCC (459 mg, 3 mmol). The reaction mixture was stirred at room temperature, and then refluxed for 10 h. The precipitates were removed by filtration through the Celite. The solution was concentrated, and the residue was washed with MeOH. The solid was purified by silica gel column chromatography (ethyl acetate/dichloromethane/petroleum ether 1:2:3), and crystallized from dichloromethane/methanol to give **7** (yield 85%) as white crystals. Mp >300 °C; ^{1}H NMR ($CDCl_3$, 600 MHz) *δ* 11.10 (s, 2H, N*H*), 10.77 (s, 2H, N*H*), 10.07 (s, 2H, N*H*), 8.40 (br s, 4H), 8.36 (br s, 2H), 8.14 (br s, 2H), 8.01 (s, 2H), 7.82 (s, 2H), 7.42−7.41 (m, *2*H), 7.26 (br, *J* = 7.4 Hz, 4H), 7.03 (d, *J* = 7.8 Hz, 2H), 6.12 (t, *J* = 7.6 Hz, 4H), 5.66 (t, *J* = 8.1 Hz, 2H), 5.54 (t, *J* = 6.8 Hz, 2H), 4.30−4.27 (m, 12H, $-OCH_2CH(CH_3)_2$), 2.50−2.40 (m, 6H, $-OCH_2CH(CH_3)_2$), 1.30−1.17 (m, $-OCH_2CH(CH_3)_2$, 36H); ^{13}C NMR ($CDCl_3$, 75 MHz) *δ* 163.4, 163.3, 162.9, 162.2, 161.9, 161.2, 151.0, 149.9, 149.6, 144.8, 144.6, 137.5, 127.5, 126.1, 123.3, 122.8, 122.7, 122.5, 122.3, 120.5, 120.4, 120.2, 119.0, 114.3, 112.8, 102.1, 101.2, 101.0, 75.7, 75.5, 28.3, 19.39, 19.36, 19.34; MALDI-TOF MS *m*/*z* 1567.9 $[M + H]^+$. Anal. Calcd for $C_{90}H_{88}F_2N_{12}O_{12}$·$2H_2O$: C, 67.40; H, 5.78; N, 10.48. Found: C, 67.39; H, 5.76; N, 10.32.

Acknowledgment. We thank the National Natural Science Foundation of China (20625206), CMS-CX200826, and National Basic Research Program of China (2007CB808004, 2008CB617501) for financial support. We also thank Prof. Eiji Yashima and co-workers at Nagoya University for doing CD experiments at various temperatures, and Dr. Hai-Bin Song at Nankai University for determining the crystal structures.

Supporting Information Available: Copies of ^{1}H and ^{13}C NMR spectra, TOCSY and NOESY spectra of **5**−**7**; CD spectra of oligoamides **1a**−**4a** in various solvents; variable-temperature ^{1}H NMR spectra of oligoamides **1**−**4** and **1a**−**4a**, variable-temperature CD spectra of oligoamides **1**, **3**, and **4** in CH_3CN and **2**−**4** in MeOH; and X-ray crystallographic files (CIF) for oligomers **3**, **3a**·CH_3OH, **3a**·H_2O, **6**, and **7**. This material is available free of charge via the Internet at http://pubs.acs.org.

JO900647D